

$^{207}\text{Pb}(p, d)^{206}\text{Pb}$ reaction and some matrix elements of the effective interaction*

W. A. Lanford and G. M. Crawley

Cyclotron Laboratory and Department of Physics, Michigan State University, East Lansing, Michigan 48823

(Received 20 August 1973)

The cross sections for the $^{207}\text{Pb}(p, d)^{206}\text{Pb}$ reaction have been measured relative to the cross sections for the $^{208}\text{Pb}(p, d)^{207}\text{Pb}$ reaction to the single-neutron-hole states in ^{207}Pb . The reactions were studied with 35-MeV protons and a final deuteron resolution of 5 keV (full width at half maximum). By making the same assumptions as are usually made in model calculations of ^{206}Pb , the matrix elements of the effective interaction of a $p_{1/2}$ neutron with neutrons in other orbits are derived from the experimental results.

[NUCLEAR REACTIONS $^{207}\text{Pb}(p, d)$, $E = 35$ MeV; measured levels, $\sigma(\theta)$; deduced S , sum rules.]

I. INTRODUCTION

There have been many calculations of the properties of ^{206}Pb .¹⁻⁵ Most of the calculations are based on the model (1) that the six states strongly excited in the $^{208}\text{Pb}(p, d)^{207}\text{Pb}$ reaction are single-neutron-hole states and (2) that ^{206}Pb can be described as two neutron holes distributed over these single-hole orbitals. The principal difference between the various calculations is in the choice of the two-body Hamiltonian which is used to describe the interaction between these neutron holes. In the analysis of the present experiment these same two basic assumptions are made. This procedure not only allows a more direct comparison of experiment with the predictions of the model calculations but also eliminates most of the usual uncertainties resulting from the distorted-wave Born-approximation (DWBA) analysis. By obtaining accurate single-nucleon-pickup strengths, sum-rule results can be usefully applied. Perhaps the most interesting sum rule (an energy-weighted sum) determines the diagonal matrix elements of the interaction of a neutron in the $p_{1/2}$ orbit with a neutron in one of the other single-neutron orbits. These experimentally determined matrix elements are compared directly with the predictions of Kuo and Herling.³ There is generally qualitative agreement, but there are also some interesting discrepancies.

The neutron-pickup spectroscopy on ^{207}Pb has been previously studied using the (d, t) reaction by Tickle and Bardwick.⁶ For the 2^+ states which can be reached by mixed- l transitions, and for weak states and close doublets, the present results are often very different from the (d, t) work.

II. EXPERIMENTAL PROCEDURE

These reactions were studied using the 35-MeV proton beam from the Michigan State University

cyclotron. The targets were isotopically enriched lead targets evaporated on $30\text{-}\mu\text{g}/\text{cm}^2$ carbon foils. The beam on the target was monitored by recording the total charge collected in the Faraday cup and by recording the protons elastically scattered at 90° with a scintillation counter (NaI). These two procedures for normalizing the relative cross section at different angles gave results which agreed to a few percent. The 90° elastic scattering monitor was used to determine the angular distributions presented here.

In the present experiment, we are principally interested in the cross sections for the $^{207}\text{Pb}(p, d)^{206}\text{Pb}$ reaction relative to the $^{208}\text{Pb}(p, d)^{207}\text{Pb}$ cross sections to the single-neutron-hole states in ^{207}Pb . While the monitoring systems accurately determined angular distributions for each individual reaction, absolute cross sections could not be obtained as accurately as the ratio of the $^{207}\text{Pb}(p, d)^{206}\text{Pb}$ cross sections to the $^{208}\text{Pb}(p, d)^{207}\text{Pb}$ cross sections. To obtain this ratio, the (p, d) reaction on a natural Pb target, for which the relative abundance of ^{207}Pb to ^{208}Pb is accurately known, was studied. This procedure allows the determination of cross sections in the $^{207}\text{Pb}(p, d)^{206}\text{Pb}$ reaction relative to cross sections in the $^{208}\text{Pb}(p, d)^{207}\text{Pb}$ reaction to a few percent.

The absolute-cross-section normalization for both reactions is more uncertain. The absolute cross section was determined in two ways: One method was to directly measure the target thickness, the spectrometer solid angle, and the charge collected in the Faraday cup, and then calculate $d\sigma/d\Omega$. The second method was to measure proton elastic scattering from $30\text{-}50^\circ$ and compare this with the cross section predicted by the optical model. The elastic scattering was measured with exactly the same particle-detection and beam-monitoring system as was used for the study of the (p, d) reactions. The optical-model param-

eters from Becchetti and Greenlees⁷ were used to predict the elastic cross section. The angular region of $30\text{--}50^\circ$ was chosen because elastic scattering has a slight peak in this region. These two techniques agreed to 5%. The uncertainty in the direct-target-thickness measurement is about 10% while the uncertainty in the elastic scattering techniques is not known. The two results were averaged, and it is expected that the absolute normalization is accurate to about 10%.

The spectra recorded for this experiment were obtained using either nuclear emulsions or a charge division position-sensitive proportional counter⁸ in the focal plane of the Michigan State University split-pole magnetic spectrograph. Sample spectra obtained with plates and with the

proportional counter are shown in Figs. 1 and 2. By making use of the high-resolution capability of the dispersion-matched cyclotron-spectrograph facility at Michigan State University, resolution of 5 keV [full width at half maximum (FWHM)] was obtained when nuclear emulsions were used to detect the deuterons. In order to obtain this resolution it was necessary to optimize the system by adjusting the dispersion of the beam across the target while monitoring the resolution with the "speculator" system.⁹ Once the dispersion was optimized, no changes were necessary throughout the experiment with no deterioration in resolution.

The proportional-counter data were taken by replacing the nuclear emulsions with a position-sensitive proportional counter. Thicker targets

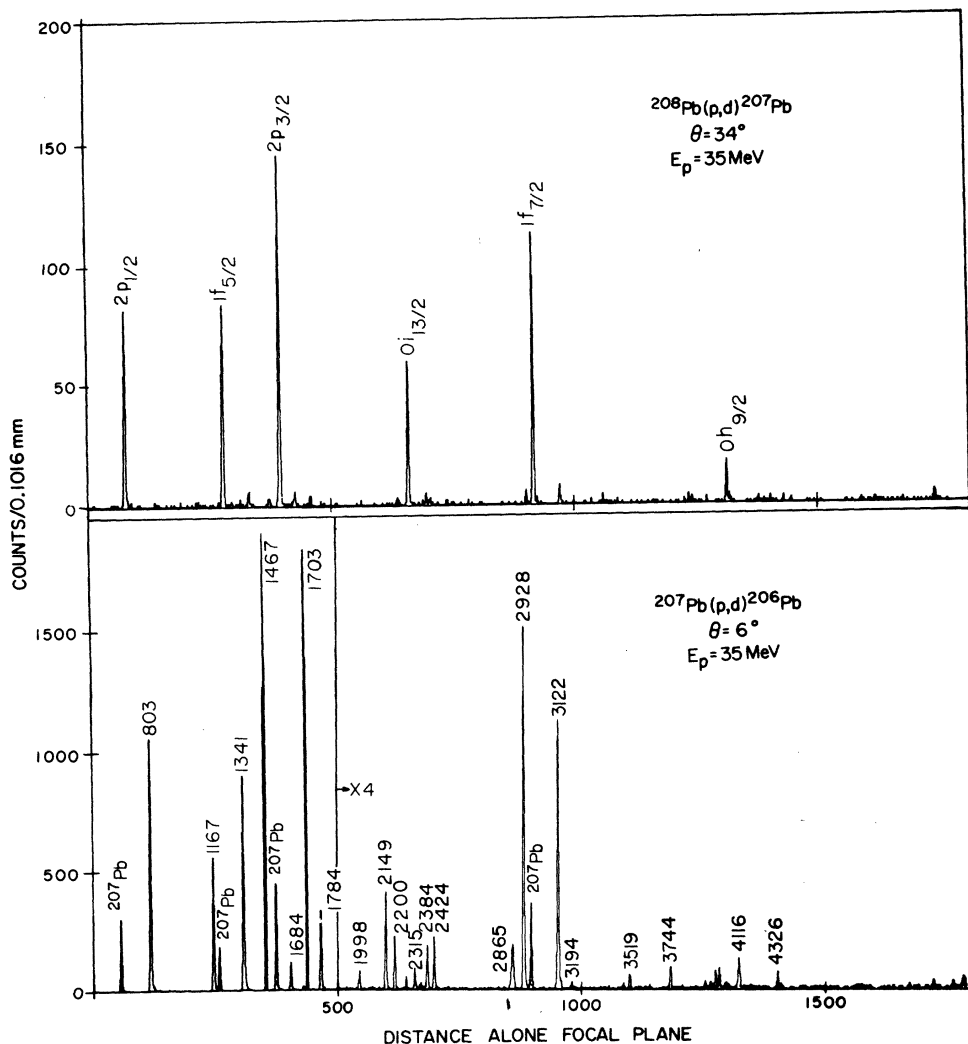


FIG. 1. Spectra of the $^{208}\text{Pb}(p,d)^{207}\text{Pb}$ and $^{207}\text{Pb}(p,d)^{206}\text{Pb}$ reactions obtained using nuclear emulsions. The resolution is about 5 keV (FWHM). The peaks in the $^{208}\text{Pb}(p,d)^{207}\text{Pb}$ spectrum are labeled by the single-hole quantum numbers. The peaks in the $^{207}\text{Pb}(p,d)^{206}\text{Pb}$ spectrum are labeled with excitation energies in keV.

(about $600 \mu\text{g}/\text{cm}^2$ as opposed to $100 \mu\text{g}/\text{cm}^2$ for plate data) were used because of the limited position resolution of the counter. These proportional-counter data have a resolution of about 45 keV (FWHM). See Fig. 2.

Each detector system has some advantages over the other. Data taken with the nuclear emulsions have far better resolution and have an accurately known calibration. Excitation energies can be determined to an accuracy of about 1 keV per 2 MeV of excitation.¹⁰ On the other hand, the proportional-counter system is an on-line device. It gives more accurate cross section data because it is not limited in the number of counts in a peak whereas plates are limited because of a maximum countable track density. In addition, there is not the uncertainty introduced by human scanning. For the present reaction study, the resolution of the proportional counter is sufficient for many of the states. For states for which 45-keV resolution is not good enough, the plate data were used. The excitation energies were determined from the plate data alone.

III. EXCITATION ENERGIES AND COMPARISON WITH LEVELS PREVIOUSLY REPORTED

The level scheme of ^{206}Pb is one of the better known of heavy nuclei. Of the 32 known levels below 3.5 MeV of excitation energy, all but 2

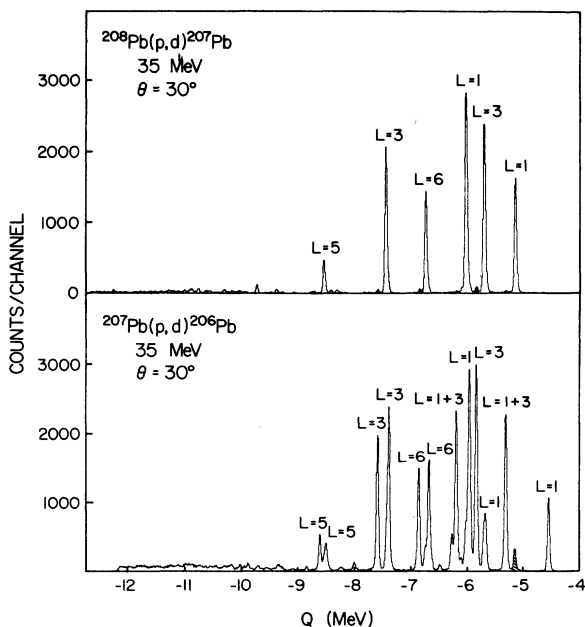


FIG. 2. Spectra of the $^{208}\text{Pb}(p,d)^{207}\text{Pb}$ and $^{207}\text{Pb}(p,d)^{206}\text{Pb}$ reactions obtained with the position-sensitive proportional counter. Both spectra were recorded at the same angle and are plotted with a common Q -value scale.

have at least tentative spin and parity assignments.¹¹ Furthermore, there is generally very good correspondence between these levels and the levels predicted by model calculations. Shown in Table I are the excitation energies of levels observed in the $^{207}\text{Pb}(p,d)^{206}\text{Pb}$ reaction. Many of the levels above 3 MeV are very weakly excited and so angular distributions to these levels could not be measured. Included in this table are states which were observed at three or more angles.

When the excitation energies of the levels in ^{206}Pb were initially determined using the calibration of the spectrometer focal plane, a systematic deviation of -2.5 keV per MeV of excitation was observed between these excitation energies and those accurately known from decay studies. It was assumed that this deviation resulted from inaccurate measurement of the beam energy and/or spectrometer field. The beam energy and spectrometer fields were adjusted in order that the levels at 0.8031, 1.3406, 1.9978, and 2.2002 MeV of excitation in ^{206}Pb have a minimum deviation, and hence a new set of excitation energies was obtained. Except for the possible systematic error introduced if the excitation energies reported by γ -decay studies have a large systematic error, the excitation energies obtained are accurate to 1 keV per 2 MeV of excitation energy.

It should be noted that there is a 2^+ level at $1467 \pm 1 \text{ keV}$ which is not in agreement with the $1459.9 \pm 0.1 \text{ keV}$ excitation reported by decay studies.¹² There is no evidence in the present experiment for a 2^+ level at 1459.9 keV and it seems unlikely that there is such a level. The authors of the decay work acknowledge experimental difficulty in measuring the γ ray associated with the proposed 1459.9-keV level.

The level at 1.703 MeV is almost certainly a 1^+ state. The evidence for this is: Since it is strongly excited with an $l=1$ angular distribution in the present experiment, it must be a 0^+ , 1^+ , or 2^+ state; it is not excited by the (p,t) reaction, indicating it has unnatural parity, i.e., 1^+ . In addition, its excitation energy, and its large single-neutron-pickup strength, is in excellent agreement with shell-model¹⁻⁴ predictions of a 1^+ state.

As can be seen in Table I and Fig. 1 there are a large number of very weakly excited states above 3.5 MeV. There are also a very large number of states reported in the literature above 3.5 MeV. In general it is difficult to associate levels seen in the present experiment with those reported by others. One possible exception is the 4^+ state at 3958 keV seen in the $^{208}\text{Pb}(p,t)^{208}\text{Pb}$ reaction¹³ which may be the 3963-keV level seen in the present experiment with an $l=3$ angular distribution.

TABLE I. Excitation energies and spin assignments in ^{206}Pb . The excitation energies and spin assignments from *Nuclear Data Sheets* and from the $^{208}\text{Pb}(p, t)^{206}\text{Pb}$ reaction include all the states below 3.5 MeV. Levels from the literature above 3.5 MeV are included only when they are likely to be the same level as observed in the present experiment.

Present experiment		Nuclear data (Ref. 11)		$^{208}\text{Pb}(p, t)^{206}\text{Pb}$ ^b		J^π adopted for analysis of present experiment
E_x ^a (MeV)	l	E_x (MeV)	J^π	E_x (MeV)	J^π	
0.0	1	0.0	0^+	0.0	0^+	0^+
0.803	1+3	0.8031	2^+	0.804	2^+	2^+
1.167	1	1.165	0^+	1.167	0^+	0^+
1.341	3	1.3406	3^+	1.339		3^+
1.467	1+3	1.4599 ^c	2^+	1.466	2^+	2^+
1.684	3	1.6841	4^+	1.684	4^+	4^+
1.703	1	1.704	(1^+)			1^+ ^c
1.784	1+3	1.784	2^+	1.784	2^+	2^+
1.998	3	1.9978	4^+	1.997	4^+	4^+
2.149	1+3	2.149	(2^+)	2.147	2^+	2^+
2.200	6	2.2002	7^-	2.199	7^-	7^-
2.315	1	2.314	(0^+)	2.314	0^+	0^+
2.384	6	2.3843	6^-	2.379		6^-
		2.3914	(4^+)			(4^+)
2.424	1+3	2.428	2^+	2.421	2^+	2^+
2.647	weak	2.6476	3^-	2.644		3^-
2.657	weak	2.6585	(9^-)	2.655		9^-
		2.7823	5^-	2.780	5^-	5^-
		2.8264	(4^-)	2.827		(4^-)
2.865	6	2.8645	7^-	2.865		7^-
2.928	3	2.93	4^+	2.928	4^+	4^+
		2.9396	6^-			6^-
		3.0165	5^-	3.014		5^-
3.122	3	3.117	$(2, 3, 4)^+$	3.119		3^+ ^c
		3.123	(6^+)			(6^+)
3.194	weak	3.191		3.193		
		3.2255	$(6, 7)^-$			
		3.2441	4^-			4^-
				3.256	5^-	5^-
		3.2793	5^-			5^-
		3.383	7^-	3.390	(7^-)	7^-
		3.4028	5^-			5^-
3.453	weak	3.452	(3)	3.452	(4^+)	$(3, 4)^+ \text{ }^d$
3.484	weak					
...
3.519	3	3.511		3.516		$(3^+, 4^+) \text{ }^d$
3.605	weak	3.610		3.603	(2^+)	
3.744	0	3.742	2			
3.963	3			3.958	4^+	4^+
3.990	(0)	3.992				
4.008	5	4.011				4^+ ^c
4.116	5			4.113		5^+
4.326	0	4326				
4.345		4340				
4.756						
4.806						
4.827						
5.038	(3)					
5.086	(3)					
5.131						
5.164						
5.194	(3)					
5.277	(0)					
5.325	(3)					

^a The excitation energies are accurate to 1 keV per 2 MeV of excitation.

^b From Ref. 13.

^c See text for comments on this level.

^d Because this level is populated with $f_{7/2}$ pickup it may be spin 3^+ or 4^+ . Both possibilities will be considered below.

Based only on the comparisons of the measured one-neutron-pickup strength and excitation energy with the shell-model predictions, it is proposed that the level at 3112 keV is 3^+ . This assignment can almost be made by inspection of Fig. 1. Since ^{207}Pb has a $p_{1/2}$ neutron hole in the ground state, the $f_{7/2}$ neutron-pickup strength will be split into 3^+ and 4^+ states with dominant configurations ($p_{1/2}^{-1} \otimes f_{7/2}^{-1}$). The 4^+ level is known to be at 2928 keV so the other strong $f_{7/2}$ transition which is at 3112 keV must have spin-parity of 3^+ . Similarly, we propose that the levels at 4008 and 4116 keV have dominant configurations of ($p_{1/2}^{-1} \otimes h_{9/2}^{-1}$) with spins 4^+ and 5^+ , respectively.

These arguments to make spin assignments based on spectroscopic strength can be put on a formal basis by invoking the dipole sum rules discussed in Sec. V below. The assignments discussed above are necessary in order that these dipole sum rules are not grossly violated.

IV. ANALYSIS

Essentially all shell-model calculations of ^{206}Pb assume that the six states strongly excited in the $^{208}\text{Pb}(p, d)^{207}\text{Pb}$ reaction are single-neutron-hole states.¹⁻⁵ That is, these six states have the configuration of one neutron hole in the $2p_{1/2}$, $1f_{5/2}$, $2p_{3/2}$, $0i_{13/2}$, $1f_{7/2}$, and $0h_{9/2}$ shell-model space. In the analysis of the $^{207}\text{Pb}(p, d)^{206}\text{Pb}$ reaction, we want to make the same assumption in order to make as direct a comparison as possible between the theory and experiment. To do this, instead of using the usual DWBA analysis to predict the angular distributions, the experimentally measured angular distributions from the study of the $^{208}\text{Pb}(p, d)^{207}\text{Pb}$ reaction to the single-neutron-hole states will be used and the cross sections for the (p, d) reaction on ^{207}Pb will be measured relative to the cross sections to these single-neutron-hole states in ^{207}Pb . Hence absolute spectroscopic factors (C^2S) for the $^{207}\text{Pb}(p, d)^{206}\text{Pb}$ reaction will not be reported, but spectroscopic factors relative to the $^{208}\text{Pb}(p, d)^{207}\text{Pb}$ reaction will be obtained. These relative spectroscopic factors will be distinguished from absolute spectroscopic factors by writing $C^2\bar{S}$ instead of C^2S .

This analysis procedure has many advantages over the conventional analysis besides obtaining $C^2\bar{S}$, which is the quantity most theories predict (not C^2S). One important advantage is that one can measure C^2S to a few percent accuracy whereas it is generally accepted that absolute spectroscopic factors can be extracted from experiment to only about 20% in the best cases. Another advantage is that, since the pure- l angular distributions are accurately known, l admixtures can

be accurately determined.

One simple test of this procedure for evaluating spectroscopic factors is to see if the angular distributions measured on ^{207}Pb are the same as those measured on ^{208}Pb . Since we are presently studying the (p, d) reaction on all the stable isotopes of lead, a more stringent test of these ideas can be made by comparing $\sigma(\theta)$ for a given angular momentum transfer as measured on all four stable isotopes. As an example, this comparison is shown for the $f_{7/2}$ transition in Fig. 3. Clearly, for all practical purposes these angular distributions are the same. Note that in Fig. 3 the curve is the same in all four cases.

A. Corrections of Q dependence in the cross section

Since the transitions in $^{207}\text{Pb}(p, d)^{206}\text{Pb}$ may occur at a different Q value from transition of the same l_j in the $^{208}\text{Pb}(p, d)^{207}\text{Pb}$ reaction, it is desirable to make corrections for such effects. Because these reactions were studied at relatively high bombarding energy and because, in almost all cases, the Q values for the reaction on different targets are nearly the same (see Fig. 2), these corrections are small, generally a few percent or less.

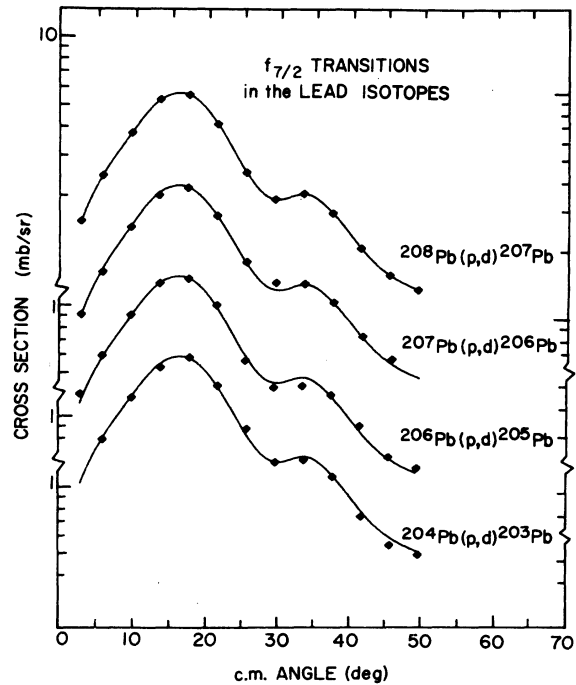


FIG. 3. Examples of $f_{7/2}$ angular distributions observed on the stable lead isotopes. The curve is the same for all four transitions. The curve is the result of interpolating between the points for the $^{208}\text{Pb}(p, d)^{207}\text{Pb}$ case and then renormalizing to fit the other cases.

To make these corrections the usual DWBA analysis of the $^{208}\text{Pb}(p, d)^{207}\text{Pb}$ reaction was made (see below) and then this DWBA description was used to make Q -value corrections in the $^{207}\text{Pb}(p, d)^{206}\text{Pb}$ reactions. While there may be 20% uncertainties in the over-all cross sections pre-

dicted by DWBA, it should be accurate to about 1% for making these small Q corrections.

B. Analysis of $^{208}\text{Pb}(p, d)^{207}\text{Pb}$ to the single-neutron-hole states

Shown in Fig. 4 are the predicted and measured angular distributions to the six single-neutron-hole states. The cross sections were calculated using the code DWUCK.¹⁴ The proton optical-model parameters are from Becchetti and Greenlees.⁷ The deuteron optical-model parameters were deduced using the Johnson-Soper model¹⁵ for (p, d) reactions. The optical-model parameters are given in Table II (in the convention used by DWUCK). As is usually the case when using the Johnson-Soper model, finite-range corrections were small. The calculation shown here used finite-range and nonlocality corrections. By examining the fits to the angular distributions, it is seen that DWBA does very well. See Fig. 4.

Since it is expected for a direct reaction that

$$\sigma_{\text{expt}}(\theta) = NC^2S \frac{\sigma_{\text{DW}}(\theta)}{(2j+1)}, \quad (4.1)$$

where $N = \frac{3}{2}D_0^2$ and D_0^2 was taken to be 1.53 for (p, d) reactions, $\sigma_{\text{DW}}(\theta)$ is the distorted-wave cross section calculated by DWUCK, and j is the angular momentum transferred, the absolute spectroscopic factors (C^2S) for the $^{208}\text{Pb}(p, d)^{207}\text{Pb}$ reaction can be deduced by varying C^2S to fit the magnitude of the cross section. The results of this analysis are given in Table III along with some other evaluations of C^2S for this reaction as previously reported.^{16, 17} We have everywhere divided C^2S by what the expected value would be if these states are pure single-neutron-hole states. As can be seen, the results are consistent with the notion that the $p_{1/2}$, $f_{5/2}$, and $p_{3/2}$ states have nearly unit spectroscopic factors while the others seem to have less. The one anomaly is the value 1.07 for

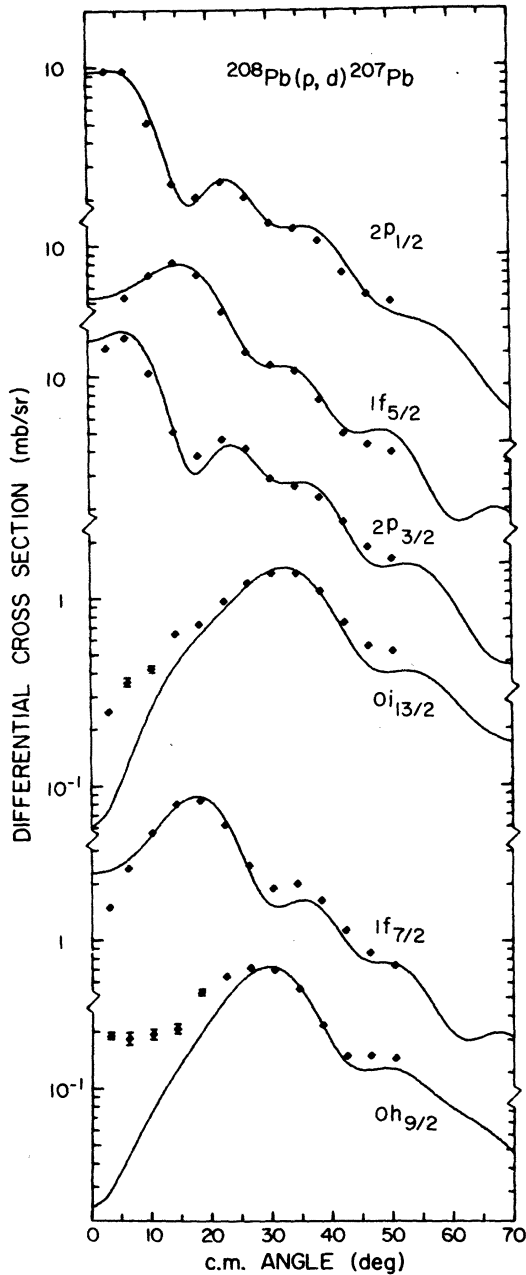


FIG. 4. Comparison of the experimental angular distribution from the $^{208}\text{Pb}(p, d)^{207}\text{Pb}$ reaction with the DWBA prediction (solid curves). The DWBA used the proton optical-model parameters from Becchetti and Greenlees with deuteron parameters determined by the Johnson-Soper model.

TABLE II. Optical-model parameters.

	Proton	Deuteron	Neutron
V (MeV)	-53.41	-105.87	
r (fm)	1.17	1.17	1.24
a (fm)	0.75	0.78	0.65
W (MeV)	-5.00	-2.30	
r' (fm)	1.32	1.29	
a' (fm)	0.658	0.653	
W_D (MeV)	22.35	65.89	
r_D (fm)	1.32	1.29	
a_D (fm)	0.658	0.647	
V_S (MeV)	-24.8	-12.40	$\lambda = 25$
r_S (fm)	1.01	1.01	1.24
a_S (fm)	0.75	0.75	0.65

the $f_{7/2}$ state¹⁷ deduced by using the Johnson-Soper model in the analysis of the Yale 22-MeV (p, d) data. It is expected that this number should be less than about 0.9 since another $f_{7/2}$ transition is observed at 4.52 MeV with about 10% of the strength of the lower $f_{7/2}$ state.

On the whole, the DWBA analysis seems rather good. We should therefore be able to make small Q -value corrections to a high accuracy.

C. Analysis of $^{207}\text{Pb}(p, d)^{206}\text{Pb}$ reaction:
The spectroscopic factors

The procedure for obtaining spectroscopic factors for the $^{207}\text{Pb}(p, d)^{206}\text{Pb}$ reaction relative to the $^{208}\text{Pb}(p, d)^{207}\text{Pb}$ reaction is now clear. We experimentally determine the cross section for $^{207}\text{Pb}(p, d)^{206}\text{Pb}$ relative to the appropriate state(s) in the $^{208}\text{Pb}(p, d)^{207}\text{Pb}$ reaction, and multiply by the Q -value correction factor and by $2j+1$ to get the relative spectroscopic factors ($C^2\tilde{S}$). The results of this procedure are shown in Table IV.

Shown in Figs. 5 and 6 are the angular distributions for the $^{207}\text{Pb}(p, d)^{206}\text{Pb}$ reaction (data points). Also included in these figures are the angular distributions measured in $^{208}\text{Pb}(p, d)^{207}\text{Pb}$ reaction (solid line). A line has been drawn between the data points measured in the $^{208}\text{Pb}(p, d)^{207}\text{Pb}$ reaction to distinguish those from the $^{207}\text{Pb}(p, d)^{206}\text{Pb}$ data. However, since both reactions were measured at the same angles and under identical experimental conditions, in the analysis the angular distributions were compared directly, point by point.

For states which can be formed by only a single l_j value (e.g. 0^+ must have $l_j = p_{1/2}$, 1^+ must have $p_{3/2}$, etc.), the measured angular distribution should be the same (up to a multiplying constant) as that seen in $^{208}\text{Pb}(p, d)^{207}\text{Pb}$. But for 2^+ states, both $p_{3/2}$ and $f_{5/2}$ transitions can contribute incoherently to the cross section. That is, one

TABLE III. Present results for spectroscopic factors to "single-hole states" in ^{207}Pb compared with other (p, d) measurements: $C^2\tilde{S}/(2j+1)$.

Orbit	Present result	Smith <i>et al.</i> ^a $E_p = 41$ MeV	Satchler's ^b analysis of 22-MeV data
$2p_{1/2}$	0.90	1.08	1.05
$1f_{5/2}$	0.86	1.05	0.98
$2p_{3/2}$	0.80	0.95	1.00
$0i_{13/2}$	0.67	0.61	0.75
$1f_{7/2}$	0.55	0.64	1.07
$0h_{9/2}$	0.49	0.68	0.70

^a Reference 16.

^b Reference 17.

expects:

$$\sigma_{\text{expt}}(\theta) = \sum_{\substack{l_j = p_{3/2} \\ \text{and } f_{5/2}}} C^2\tilde{S}(l_j) \frac{\sigma^{l_j}(\theta)(208)}{(2j+1)}, \quad (4.2)$$

where $\sigma^{l_j}(\theta)(208)$ stands for the cross section measured in the $^{208}\text{Pb}(p, d)^{207}\text{Pb}$ reaction. In order to obtain this l admixture, a simple least-squares fitting was made to obtain $C^2\tilde{S}(p_{3/2})$ and $C^2\tilde{S}(f_{5/2})$. The fits obtained can be seen in Figs. 5 and 6 for the states at 0.803, 1.467, 1.784 MeV, etc. The least-squares-fitting program also deduces the

TABLE IV. $^{207}\text{Pb}(p, d)^{206}\text{Pb}$ spectroscopic factors, relative to $^{208}\text{Pb}(p, d)^{207}\text{Pb}$.

J^π	E (MeV)		l_j	$C^2\tilde{S}$	
	Expt	Calc ^a		Expt ^b	Calc ^a
0^+	0.0	0.0	$p_{1/2}$	0.59	0.52
2^+	0.803	0.89	$p_{3/2}$	0.42(0.04)	0.65
			$f_{5/2}$	1.64(0.07)	1.40
0^+	1.167	1.16	$p_{1/2}$	0.37	0.41
3^+	1.341	1.38	$f_{5/2}$	3.54	3.50
2^+	1.467	1.39	$p_{3/2}$	1.52(0.06)	1.57
			$f_{5/2}$	0.64(0.09)	0.80
4^+	1.684	1.81	$f_{7/2}$	0.17	0.21
1^+	1.703	1.68	$p_{3/2}$	1.53	1.50
2^+	1.784	1.82	$p_{3/2}$	0.27(0.02)	0.13
			$f_{5/2}$	0.02(0.01)	0.10
4^+	1.998	2.05	$f_{7/2}$	0.14	0.06
2^+	2.149	2.25	$p_{3/2}$	0.077(0.006)	0.04
			$f_{5/2}$	0.034(0.010)	0.06
7^-	2.200		$i_{13/2}$	7.05	7.00
0^+	2.315	2.33	$p_{1/2}$	0.021	0.075
6^-	2.384		$i_{13/2}$	6.47	6.45
2^+	2.424	2.41	$p_{3/2}$	0.044(0.004)	
			$f_{5/2}$	0.014(0.008)	
7^-	2.865		$i_{13/2}$	0.32	0.38
4^+	2.928	2.98	$f_{7/2}$	3.97	3.96
3^+	3.122	3.10	$f_{7/2}$	3.37	3.50
$(3^+, 4^+)$	3.519		$f_{7/2}$	0.21	
			$l=0$		
4^+	3.744		$f_{7/2}$	0.076	
			$(l=0)$		
4^+	3.963		$h_{9/2}$	4.30	
5^+	4.008	4.33	$h_{9/2}$	5.00	5.44
			$l=0$		
	4.326		$(f_{7/2})$	(0.061)	
	5.038		$(f_{7/2})$	(0.075)	
	5.086		$(f_{7/2})$	(0.076)	
	5.194		$(l=0)$		
	5.277		$(f_{7/2})$	(0.207)	
	5.325		$(f_{7/2})$		

^a In addition to the levels listed, there are predicted 1^+ and 3^+ levels at about 2.2 MeV. However, these levels have predicted spectroscopic factors of order 10^{-3} and so should not be seen (Ref. 1).

^b The numbers in parentheses for 2^+ states are the errors in the spectroscopic factors as derived from the least-squares fitting of the 2^+ angular distributions.

uncertainty in the spectroscopic factors. These errors are given in Table IV for the 2^+ states. Generally, the fits are excellent and, since the shapes of the $p_{3/2}$ and $f_{5/2}$ angular distributions are rather different, the mixtures are well determined.

In general, the experiment and analysis procedure allows us to deduce values of C^2S accurate to about $\pm 5\%$ for the strong states. For the weak states, there is more uncertainty simply because of poor statistics. For the weak states there may

also be contributions to the cross section from other than direct one-step neutron pickup. The size of such effects can be estimated by looking at the weak states excited in the $^{206}\text{Pb}(p, d)^{207}\text{Pb}$ reaction. For example, there is at 2.622 and 2.658 MeV in ^{207}Pb a doublet believed to have the configuration of a $p_{1/2}$ neutron hole coupled to the 3^- state in ^{208}Pb . These states are not expected to be excited by direct one-step single-neutron pickup, but they may be excited by a two-step process of inelastic scattering to the 3^- , then neutron pickup.

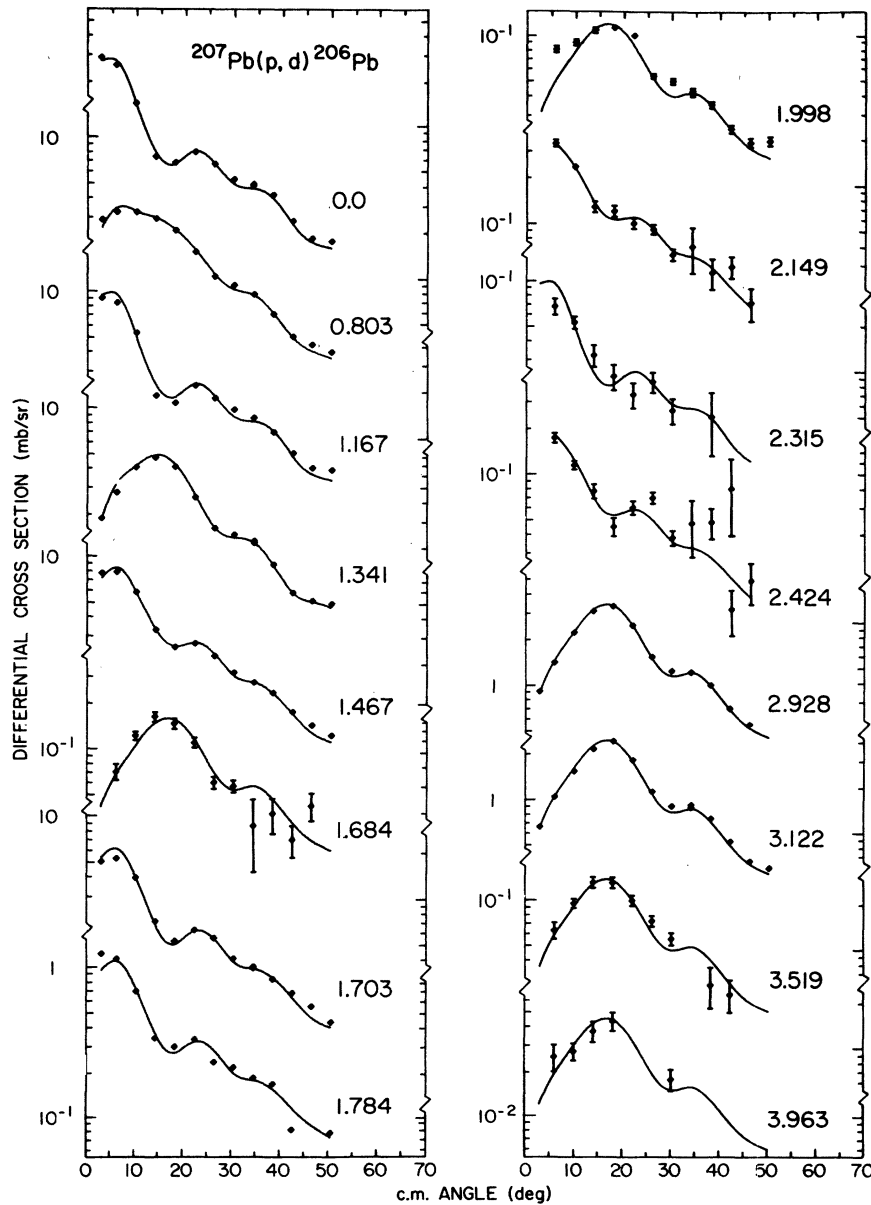


FIG. 5. Angular distributions for the $^{207}\text{Pb}(p, d)^{206}\text{Pb}$ reaction. Included are all the $l=1$ and $l=3$ transitions to states below 5 MeV. The solid curve represents the angular distributions as determined from the $^{208}\text{Pb}(p, d)^{207}\text{Pb}$ reaction.

The peak cross section to the doublet was measured to be about $25 \mu\text{b}/\text{sr}$ which is small compared with most of the transitions used in the analysis of the $^{207}\text{Pb}(p, d)^{206}\text{Pb}$ reaction. See Figs. 5 and 6. Hence, two-step processes are not expected to have much effect on the analysis of the $^{207}\text{Pb}(p, d)^{206}\text{Pb}$ reaction.

Also shown in Table IV are the shell-model predictions of McGrory *et al.*¹ If the spectroscopic factors in Table IV had been deduced by a conventional DWBA analysis and consequently had been accurate to 20 or 30%, the agreement between experiment and theory would be considered almost perfect. However, since the C^2S values are generally accurate to about 5%, it is seen that there are discrepancies outside the errors. It is

hoped that comparing accurately determinable quantities such as the C^2S in Table IV with model predictions will help in the improvement of the models.

V. SUM RULES

The following notation will be used: Let the angular momentum of the target be denoted j_0 , the angular momentum of the final state in the residual nucleus be denoted J , and the orbital and total angular momentum of the transferred nucleon be denoted l_j . In the summations discussed below, all sums will be over transitions to all the states populated with l_j unless the J_{final} of the state is specified; then the sum is over all states with spin J populated with angular momentum l_j .

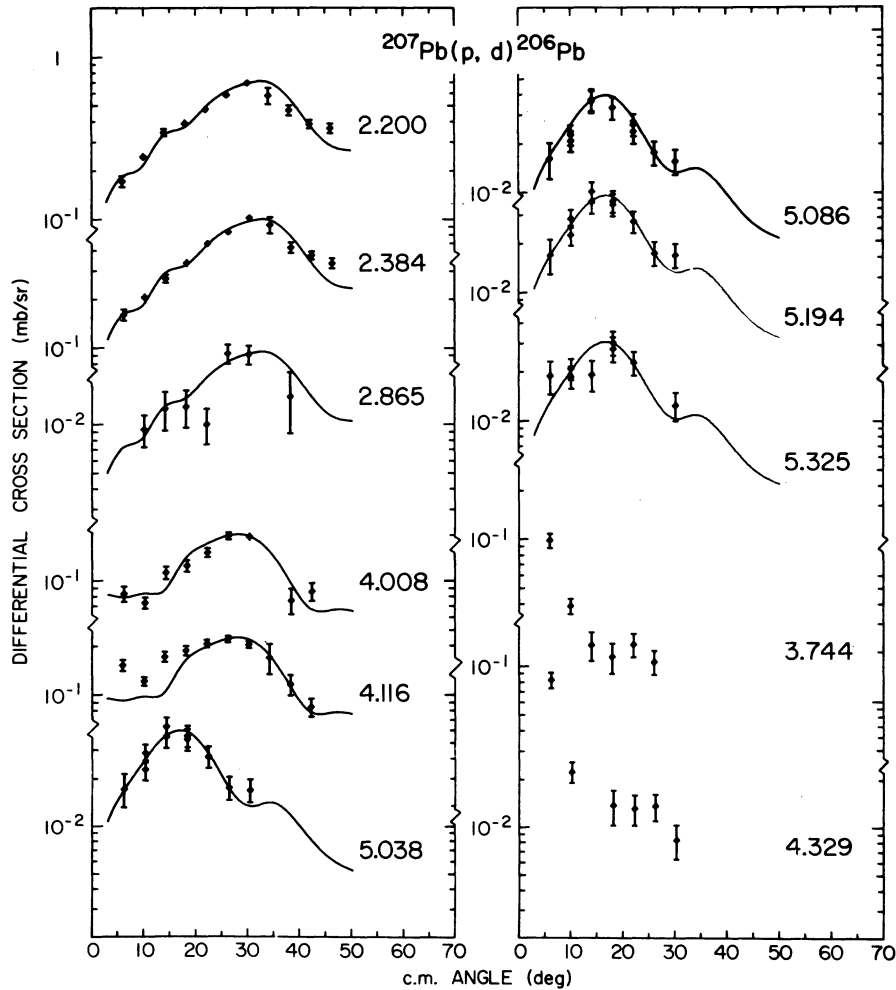


FIG. 6. Angular distributions for the $^{207}\text{Pb}(p, d)^{206}\text{Pb}$ reaction. Included are the $l=0, 5,$ and 6 transitions and the $l=3$ transitions to states above 5 MeV of excitation. The curve is the angular distribution as measured in the $^{208}\text{Pb}(p, d)^{207}\text{Pb}$ reaction. There is no curve for the $l=0$ transitions. They are identified by the strong forward peaking which is predicted by DWBA.

A. Monopole sum rule

The usual monopole sum rule when applied to nuclei with a large neutron excess (such that all the l_j orbits involved are empty of protons) is:

$$g^0(l_j) \equiv \sum C^2 \tilde{S}(l_j) = \text{number of neutrons in orbit } l_j \text{ of the target.} \quad (5.1)$$

The results of evaluating these summations for the $^{207}\text{Pb}(p, d)^{206}\text{Pb}$ reaction are shown in Table V. As can be seen, to a few percent accuracy the total sum-rule strength has been observed. It should be pointed out that in the $f_{7/2}$ sum, only the transitions to states below 5.0 MeV of excitation were included. There were some weak $l=3$ transitions observed above 5 MeV at about the same Q value as the fragment of $f_{7/2}$ strength seen at 4.52 MeV in the $^{208}\text{Pb}(p, d)^{207}\text{Pb}$ reaction. It seems likely that these high-lying $l=3$ transitions have strengths originating from the high-excitation fragment of $f_{7/2}$ strength seen in the (p, d) reaction on ^{208}Pb . Since only the low-lying state was included in the $f_{7/2}$ strength from the $^{208}\text{Pb}(p, d)^{207}\text{Pb}$ reaction, only the strength below 5 MeV was used in evaluating the $f_{7/2}$ sum rules.

The fact that to a few percent the full monopole sum-rule strength has been found in the $^{207}\text{Pb}(p, d)^{206}\text{Pb}$ reaction indicates that comparison of individual transition strengths with shell-model predictions should provide a critical test of the calculations, whereas a conventional DWBA analysis which would give C^2S 's accurate to about $\pm 20\%$ would provide a very crude test. In addition, since the full monopole strength is observed, higher-order sum rules may also be useful.

B. Fixed J_{final} (dipole) sum rules

Since most of the states excited in the $^{207}\text{Pb}(p, d)^{206}\text{Pb}$ reaction have known spins, it is of interest to consider sum rules which sum over transitions with both fixed l_j and fixed J_{final} . While these sum

TABLE V. The monopole sum-rule results for the $^{207}\text{Pb}(p, d)^{206}\text{Pb}$ reaction.

Orbit	$g^0(l_j)$	Sum-rule limit	Ratio = $\frac{g^0(l_j)}{\text{limit}}$
$p_{1/2}$	0.98	1.00	0.98
$f_{5/2}$	5.89	6.00	0.98
$p_{3/2}$	3.86	4.00	0.97
$i_{13/2}$	13.84	14.00	0.99
$f_{7/2}$	7.94	8.00	0.99
$h_{9/2}$	9.30	10.00	0.93

rules are not new,¹⁸ they do not seem to be well known, so a brief derivation of the sum rules needed will be given. Let the basis states of two neutron holes outside the ^{206}Pb core be denoted $|\alpha J^\pi\rangle$. When the residual interaction between these basis states is included, they mix to form the wave functions of states in ^{206}Pb (denoted $|\beta J^\pi\rangle$). The usual shell-model calculation is used to write $|\beta J^\pi\rangle$ as an expansion in the basis state $|\alpha J^\pi\rangle$. However, the basis state $|\alpha J^\pi\rangle$ can also be written as an expansion in the wave functions of ^{206}Pb :

$$|\alpha J^\pi\rangle = \sum_{\beta} \langle \beta | \alpha \rangle |\beta J^\pi\rangle. \quad (5.2)$$

But since the target is assumed to be a pure $p_{1/2}$ neutron hole outside a ^{208}Pb closed core, we know the total l_j pickup strength to the states $|\alpha J^\pi\rangle$ which have the form $|p_{1/2}^{-1} l_j^{-1} J^\pi\rangle$. The total l_j pickup strength $[g^0(l_j)]$ is split into states with the various possible J_{final} values with strengths (1) proportional to $2J+1$ and (2) still preserving the monopole strengths discussed above. Since

$$\sum_{J=J_1-J_2}^{J_1+J_2} (2J+1) = (2j_1+1)(2j_2+1),$$

it follows that the pickup strength to states with the same J_{final} is given by:

$$\begin{aligned} g^1(l_j, J) &\equiv \sum C^2 \tilde{S}(l_j, J) = \frac{2J+1}{(2j+1)(2j_0+1)} g^0(l_j) \\ &= \frac{2J+1}{(2j+1)(2j_0+1)} \left(\text{number of neutrons in} \right) \\ &\quad \left(\text{orbit } l_j \text{ of target} \right). \end{aligned} \quad (5.3)$$

TABLE VI. Dipole sum-rule results for the $^{207}\text{Pb}(p, d)^{206}\text{Pb}$ reaction.

Orbit	J_{final}	$g^1(l_j, J)$	Sum-rule limit	Ratio = $\frac{g^1(l_j, J)}{\text{limit}}$
$p_{1/2}$	0^+	0.98	1.00	0.98
$f_{5/2}$	2^+	2.35	2.50	0.94
	3^+	3.54	3.50	1.01
$p_{3/2}$	1^+	1.53	1.50	1.02
	2^+	2.33	2.50	0.93
$i_{13/2}$	6^-	6.47	6.50	0.99
	7^-	7.37	7.50	0.98
$f_{7/2}$	3^+	3.58(3.37) ^a	3.50	1.02 (0.96) ^a
	4^+	4.36(4.57) ^a	4.50	0.97 (1.01) ^a
$h_{9/2}$	4^+	4.30	4.50	0.96
	5^+	5.00	5.50	0.91

^a These are the values obtained assuming the state at 3.519 MeV is 4^+ , not 3^+ .

Of course, this is the expected result if the transferred neutron is only weakly coupled to the $p_{1/2}$ neutron hole in the target, but because of Eq. (5.2) Eq. (5.3) is true regardless of the residual interaction mixing the two-neutron-hole states of ^{206}Pb .

The results of applying this dipole sum rule are shown in Table VI. As mentioned above and as shown in Table I, most of the states excited have at least tentative spin assignment. However, the level at 3.519 ($f_{7/2}$) has no spin assignments. In principle this spin could be assigned by requiring the experimental dipole sums to equal the sum-rule limit. However, in the present case the experimental accuracy is not sufficient for this assignment to be made. The results assuming the alternate spin assignment are shown in parentheses and footnoted in Table VI.

C. Linear energy-weighted sum rule

Because of Eq. (5.2), some matrix elements of the interaction Hamiltonian between the two-neutron-hole states can be evaluated. Let H be this interaction such that $H|\beta J^\pi\rangle = E_\beta(J^\pi)|\beta J^\pi\rangle$, where $E_\beta(J^\pi)$ is the energy of state β in ^{206}Pb . Using Eq. (5.2), it follows:

$$\langle\alpha J^\pi|H|\alpha J^\pi\rangle = \sum_{\beta} |\langle\beta|\alpha\rangle|^2 E_\beta(J^\pi). \quad (5.4)$$

By studying the (p, d) reaction on ^{208}Pb (a closed core) and ^{207}Pb (a $p_{1/2}$ neutron hole outside the core), the expansion coefficients $|\langle\beta|\alpha\rangle|^2$ of Eq.

(5.4) can be deduced for basis states $|\alpha J^\pi\rangle$ of the form $|p_{1/2}^{-1}l_j^{-1}J^\pi\rangle$. To within a normalization (by definition) they are just the spectroscopic factors, i.e., $|\langle\beta|p_{1/2}^{-1}l_j^{-1}J^\pi\rangle|^2 \cong C^2\bar{S}(l_j\beta)$, where $C^2\bar{S}(l_j\beta)$ is the spectroscopic factor to state β in ^{206}Pb . Then, using Eq. (5.4) and putting in the normalization,

$$\begin{aligned} \epsilon^1(l_j J) &= \frac{\sum_{\beta} C^2\bar{S}(l_j\beta)E_\beta(J)}{g^1(l_j J)} \\ &= \langle p_{1/2}^{-1}l_j^{-1}J|H|p_{1/2}^{-1}l_j^{-1}J\rangle. \end{aligned} \quad (5.5)$$

The above matrix element is for the total interaction H . Usually it is the two-body part which is predicted by theories of the effective interaction in nuclei, and the zero- and one-body parts are taken from experiment. The pure two-body part of Eq. (5.5) can be deduced by subtracting the single-particle energies as obtained from the masses of ^{208}Pb , ^{207}Pb , and the single excitations of the single-particle states in ^{207}Pb .

Shown in Table VII are the results of evaluating $\langle p_{1/2}^{-1}l_j^{-1}J|H|p_{1/2}^{-1}l_j^{-1}J\rangle$ from Eq. (5.5). Also shown in this table are the two-body matrix elements deduced by subtracting the single-particle energies. These two-body matrix elements are compared with the matrix elements predicted by Kuo and Herling.³

While most of the states in ^{206}Pb which are excited in the (p, d) reaction have known spins, there are a few which are uncertain (see discussion in Sec. III). Hence it is also of interest to sum over all states excited with the same l_j .

TABLE VII. Linear energy-weighted (dipole) sum-rule results from the $^{207}\text{Pb}(p, d)^{206}\text{Pb}$ reaction.

Orbit	J	$\epsilon^1(l_j J)$ (MeV)	Single-particle energy (MeV)	$\langle p_{1/2}^{-1}l_j^{-1}J H_{12} p_{1/2}^{-1}l_j^{-1}J\rangle$ (MeV)	
				Experiment	Kuo and Herling (Ref. 3)
$p_{1/2}$	0^+	0.490	0.640	-0.150	-0.165
$f_{5/2}$	2^+	1.020	1.210	-0.190	-0.146
	3^+	1.341	1.210	+0.131	+0.067
$p_{3/2}$	1^+	1.703	1.538	+0.165	0.035
	2^+	1.425	1.538	-0.113	0.042
$i_{13/2}$	6^-	2.385	2.273	+0.114	0.090
	7^-	2.229	2.273	-0.044	-0.036
$f_{7/2}$	3^+	3.154(3.122) ^a	2.980	+0.165(+0.142) ^a	+0.006
	4^+	2.868(2.898) ^a	2.980	-0.112(-0.082) ^a	-0.153
$h_{9/2}$	4^+	4.008	4.049	-0.041	-0.054
	5^+	4.109	4.049	+0.060	+0.109

^a These values are obtained assuming the state at 3.519 MeV is 4^+ , not 3^+ .

It then follows from Eq. (5.5) and since $\sum_J g^1(l_j, J) = g^0(l_j)$,

$$\epsilon^0(l_j) \equiv \frac{\sum C^2 \bar{S}(l_j, \beta) E_\beta}{g^0(l_j)} = \frac{\sum (2J+1) \langle \alpha J | H | \alpha J \rangle}{\sum (2J+1)}$$

While this sum contains no information not contained in Eq. (5.5), it can be evaluated without knowing the J_{final} 's and so is more certain than Eq. (5.5). Again subtracting the single-particle energies, these two-body matrix elements are shown in Table VIII along with the predictions of Kuo and Herling.³

VI. DISCUSSION OF THE RESULTS

A. Non-energy-weighted sum rules

In the present experiment, the monopole and dipole sum rules can be used to test the quality of the experimental results (and the assumptions made in the analysis). As discussed in Sec. II, it is expected that the absolute values of the $C^2 \bar{S}$'s are accurate to about $\pm 5\%$ except for the mixed- l transitions to 2^+ states and for the very weak transitions. This conclusion is verified by the comparison of the sum rules shown in Tables V and VI. The ratio of the experimental monopole sum (which does not depend on knowing any J_{final} 's to the sum-rule limit is within 2% of 0.98, except for the $h_{9/2}$ orbit. See Table V.

Examination of the dipole sum-rule results further confirms the accuracy of the experimental procedure and analysis. Here the ratio of the experimental sums to the sum-rule limit is generally within 5% of 0.98. (See Table VI.) This agreement also indicates that the summary of spin assignments given in Table I is correct for the states strongly excited in the (p, d) reaction. Notice that changing the spin assignments of the levels at 1.703, 3.112, 4.008, and 4.116 MeV and then reevaluating the dipole sum rules would indeed cause violent disagreement between experiment and the sum-rule limit. For example if the level at 1.703 MeV was assigned 2^+ not 1^+ , the

TABLE VIII. Linear energy-weighted (monopole) sum-rule results for the $^{207}\text{Pb}(p, d)^{206}\text{Pb}$ reaction.

Orbit	$\epsilon^0(l_j)$ (MeV)	Single-particle energy (MeV)	Two-body centroid ^a	
			Experiment (MeV)	Kuo and Herling (Ref. 3) (MeV)
$p_{1/2}$	0.490	0.640	-0.150	-0.165
$f_{5/2}$	1.214	1.210	+0.004	-0.022
$p_{3/2}$	1.535	1.538	-0.003	0.040
$i_{13/2}$	2.301	2.273	+0.028	0.022
$f_{7/2}$	2.993	2.980	+0.013	-0.083
$h_{9/2}$	4.065	4.049	+0.016	0.025

^a Negative sign means attractive.

$p_{3/2}$ dipole sum rule for $J=2$ would be exceeded by almost 100% while the $J=1$ sum rule would not be fulfilled.

B. Linear energy-weighted sum rule

The simplest and most accurately measurable energy sum rule is the monopole sum. The result of this summation is sometimes referred to as the center of gravity of the interaction or average interaction, in this case of the $p_{1/2}$ neutron with a neutron in orbit l_j . The most striking feature shown in the evaluation of $\epsilon^0(l_j)$ is that the average interaction between a $p_{1/2}$ neutron and a neutron in a different orbit is small compared with the individual matrix elements of the interaction. As can be seen in Tables VII and VIII most of the individual matrix elements have a magnitude of order 150 keV while the average interaction is of order 10 keV. The case with two neutrons in the same orbit is special not only because the Pauli principle allows only the J -even states but also the "pairing" nature of the nucleon-nucleon force results in a large negative $J=0$ matrix element. Both of these effects result in a monopole sum for the $p_{1/2}$ orbit which is both large and negative compared with the small values for the other orbits.

The matrix elements from experiment seem to display some systematic features:

- (1) As mentioned above, the J -averaged interaction is small compared with the individual matrix elements.
- (2) Since there are just two possible J values for each orbit (because the target spin is $\frac{1}{2}$), one matrix element is positive and one is negative with magnitudes of each such that (1) holds.
- (3) Which of the two matrix elements is positive and which is negative is determined by whether Nordheim's number ($n = l_1 + l_2 + j_1 + j_2$) is even or odd. For all cases where n is odd, the matrix element with lower J is negative; when n is even, the lower- J matrix element is positive.

Perhaps the most interesting result in Tables VII and VIII is the comparison of the individual matrix elements of the effective interaction with those calculated by Kuo from a Hamada-Johnston potential and renormalized with a one-particle-three-hole core-polarization correction. With a few notable exceptions there is general agreement between Kuo's predictions and the matrix elements determined from experiment. In particular, the J average of Kuo's matrix elements are relatively small compared with the individual matrix elements. Also, the individual matrix elements have the same sign as those from experiment, except for $\langle p_{1/2}^{-1} p_{3/2}^{-1} J=2 | H_{12} | p_{1/2}^{-1} p_{3/2}^{-1} J=2 \rangle$.

In addition, there do seem to be some discrepancies in the magnitudes for

$$\langle p_{1/2}^{-1}p_{3/2}^{-1}J=1, 2 | H_{12} | p_{1/2}^{-1}p_{3/2}^{-1}J=1, 2 \rangle$$

and

$$\langle p_{1/2}^{-1}f_{7/2}^{-1}J=3 | H_{12} | p_{1/2}^{-1}f_{7/2}^{-1}J=3 \rangle.$$

There are no experimental effects which might single out these matrix elements and result in a greater uncertainty in their experimental determination. In addition, the fact that the experimental matrix elements all exhibit the systematics mentioned above would tend to indicate that the problem may be with the calculation. It would be of interest to see if these particular matrix elements have any special features in the calculations which might explain why they are different from the systematics of the other matrix elements. This discrepancy for the $p_{1/2}f_{7/2}$ matrix elements also shows up in the centroid shown in Table VIII.

C. Comparison of individual transition strengths with model predictions

There have been many calculations of the properties of ^{206}Pb .¹⁻⁵ Comparison between experiment and predicted $C^2\tilde{S}$ will be made for a sample of four of these calculations:

(1) The shell-model calculations of McGrory *et al.*¹

which predict the spectra and wave functions for ^{204}Pb , ^{205}Pb , and ^{206}Pb using the same model assumptions. These calculations use a complete six-orbit basis and a two-body interaction based on the calculated matrix elements of Kuo. The interaction was modified by changing the strength of the renormalization correction to improve agreement between experimental spectra and theory.

(2) The shell-model calculations of Ma and True² are similar to calculation (1) but use a purely phenomenological interaction.

(3) The calculations of Kuo and Herling³ are also similar to (1) except that the calculated matrix elements have not been modified but use the full renormalization correction.

(4) The calculations of Vary and Ginocchio⁴ use the two-nucleon random-phase approximation. Because these are not exact shell-model calculations, a much larger basis could be used.

Comparison between experiment and theory is shown in Fig. 7. The shaded bar is experiment and the four unshaded bars are the predictions of calculations (1)–(4) (from left to right, respectively). There are several interesting features shown in Fig. 7. Note that for the very strong transitions (say $C^2\tilde{S} \geq 1.5$) there is generally ex-

cellent agreement between experiment and all four predictions. This result follows from the fact that most of these states have very simple and rather pure configurations simply because there are not many other configurations with the same J^π with which these states can mix. For example, there are very few ways to make 1^+ , 3^+ , 6^- , or 7^- states. Hence it is not surprising that all calculations give the same results. It is interesting that for these cases where all four predictions are essentially the same, there is excellent agreement with experiment.

For moderate transition strengths (say $0.5 < C^2\tilde{S} < 1.5$), the predictions vary about $\pm 20\%$ for the different theories. There is no very strong correlation between the experiment and any one of the theories, but, on the other hand, all four agree with experiment to about 20% accuracy. For

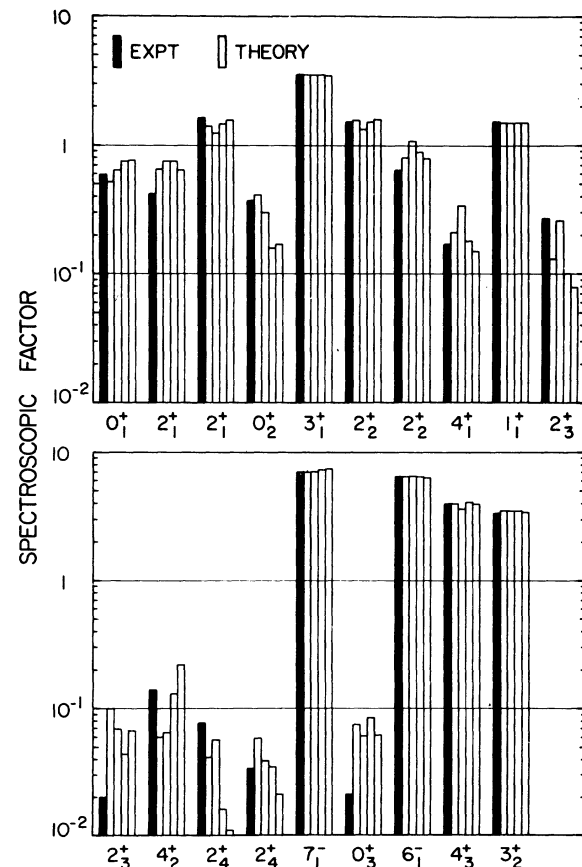


FIG. 7. Comparison of the experimental spectroscopic factors with predictions of various theories. The theoretical predictions are (left to right) those of McGrory *et al.* (Ref. 1), Ma and True (Ref. 2), Kuo and Herling (Ref. 3), and Vary and Ginocchio (Ref. 4). The transitions are labeled by the spin and parity of the final states. For transitions to 2^+ states, spectroscopic factors for both $p_{3/2}$ and $f_{5/2}$ transitions are given.

transitions with $C^2\bar{S} < 0.5$, the various theories give very different predictions, sometimes differing from each other by almost an order of magnitude. Again, the various predictions usually bracket the experimental result, but no one of the theories is clearly seen to be superior to the others.

It is interesting to note that the calculations which give the best agreement for spectra [McGrory *et al.* and Ma and True—calculations (1) and (2), respectively] do not give very much better predictions for the spectroscopic factors. This is perhaps a reflection of the variational principle which states that, to first order, a small change in the interaction Hamiltonian changes only the energy eigenvalues, not the wave functions.

The fact that the model predictions do not seem to maintain detailed agreement with experiment for other than the strongest transitions indicated that the present set of experimental results can be fruitfully used to test new models in a very straightforward way. Since the various predictions do fluctuate about experiment, it seems possible that the basic model assumptions are essentially correct but that details of the interaction (or perhaps the basis states) need some modifications.

VII. CONCLUSIONS

The present results demonstrate that by making use of the assumptions (1) that the six states

strongly excited in the $^{208}\text{Pb}(p, d)^{207}\text{Pb}$ reaction are "single-neutron-hole" states and (2) that the low-lying states in ^{206}Pb can be described as two-neutron-hole states, so that the $^{207}\text{Pb}(p, d)^{206}\text{Pb}$ results are then naturally compared with the $^{208}\text{Pb}(p, d)^{207}\text{Pb}$ results, one can avoid most of the problems associated with the usual uncertainty in DWBA analysis. In particular, one can measure relative spectroscopic factors ($C^2\bar{S}$) to a few percent accuracy. Having accurate spectroscopic information then allows not only a meaningful comparison with model calculations, but also makes sum-rule results accurate and consequently interesting. In order that fixed J_{final} sum rules (dipole) can be applied, it is necessary to know the final spins of the states excited, but for ^{206}Pb this is generally the case. Perhaps the most interesting sum-rule results are those shown in Tables VII and VIII, where the results of energy-weighted sum rules are compared with the predictions of Kuo for the strength of interaction between a $p_{1/2}$ neutron and a neutron in any of the six orbits in this major shell. Aside from a few interesting discrepancies there is generally qualitative agreement between the matrix element deduced from the present experiment and those calculated from the Hamada-Johnston potential with corrections for core polarizations.

The authors would like to thank J. McGrory and T. T. S. Kuo for communicating unpublished results and W. Benenson for helpful comments on this manuscript.

*Work supported by the National Science Foundation.

¹J. B. McGrory, A. Arima, C. M. Ko, T. T. S. Kuo, and G. Herling, *Bull. Am. Phys. Soc.* **17**, 579 (1972); private communications.

²C. W. Ma and W. W. True, University of California at Davis, Report, 1973 (to be published).

³T. T. S. Kuo and G. H. Herling, Naval Research Laboratory Report No. 2258, 1971 (unpublished); private communication.

⁴J. Vary and J. N. Ginocchio, *Nucl. Phys.* **A166**, 479 (1971).

⁵N. Freed and W. Rhodes, *Nucl. Phys.* **A126**, 481 (1969).

⁶R. Tickle and J. Bardwick, *Phys. Rev.* **166**, 1167 (1968).

⁷F. D. Becchetti and G. W. Greenlees, *Phys. Rev.* **182**, 1190 (1969).

⁸W. A. Lanford, W. Benenson, G. M. Crawley, E. Kashy, I. D. Proctor, and W. F. Steele, *Bull. Am. Phys. Soc.* **17**, 895 (1972); H. W. Fulbright, R. G. Markham, and W. A. Lanford, *Nucl. Instrum. Methods* **108**, 125 (1973).

⁹H. G. Blosser, G. M. Crawley, R. deForest, E. Kashy, and B. H. Wildenthal, *Nucl. Instrum. Methods* **91**, 61 (1971).

¹⁰E. Kashy, I. D. Proctor, J. A. Nolen, and S. Ewald,

Bull. Am. Phys. Soc. **17**, 483 (1972).

¹¹K. K. Seth, *Nucl. Data* **B7**, 161 (1972).

¹²J. C. Manthuruthil, D. C. Camp, A. V. Ramayya, J. H. Hamilton, J. J. Pinajian, and J. W. Doornebos, *Phys. Rev. C* **6**, 1870 (1972).

¹³W. A. Lanford, to be published.

¹⁴P. D. Kunz, University of Colorado, private communication.

¹⁵R. Johnson and P. J. R. Soper, *Phys. Rev. C* **1**, 976 (1970).

¹⁶S. M. Smith, P. G. Roos, C. Moazed, and A. M. Bernstein, *Nucl. Phys.* **A173**, 32 (1971).

¹⁷G. R. Satchler, *Phys. Rev. C* **4**, 1485 (1971). The data which were analyzed are from C. A. Whitten, N. Stein, G. E. Holland, and D. A. Bromley, *Phys. Rev.* **188**, 1941 (1969).

¹⁸R. M. Bansal and J. B. French, *Phys. Lett.* **19**, 223 (1965); J. B. French, in *Many-Body Description of Nuclear Structure and Reactions, Proceedings of the International School of Physics "Enrico Fermi," Course XXXVI, 1966*, edited by C. Bloch (Academic, New York, 1966); lectures given at University of Rochester 1969-71.